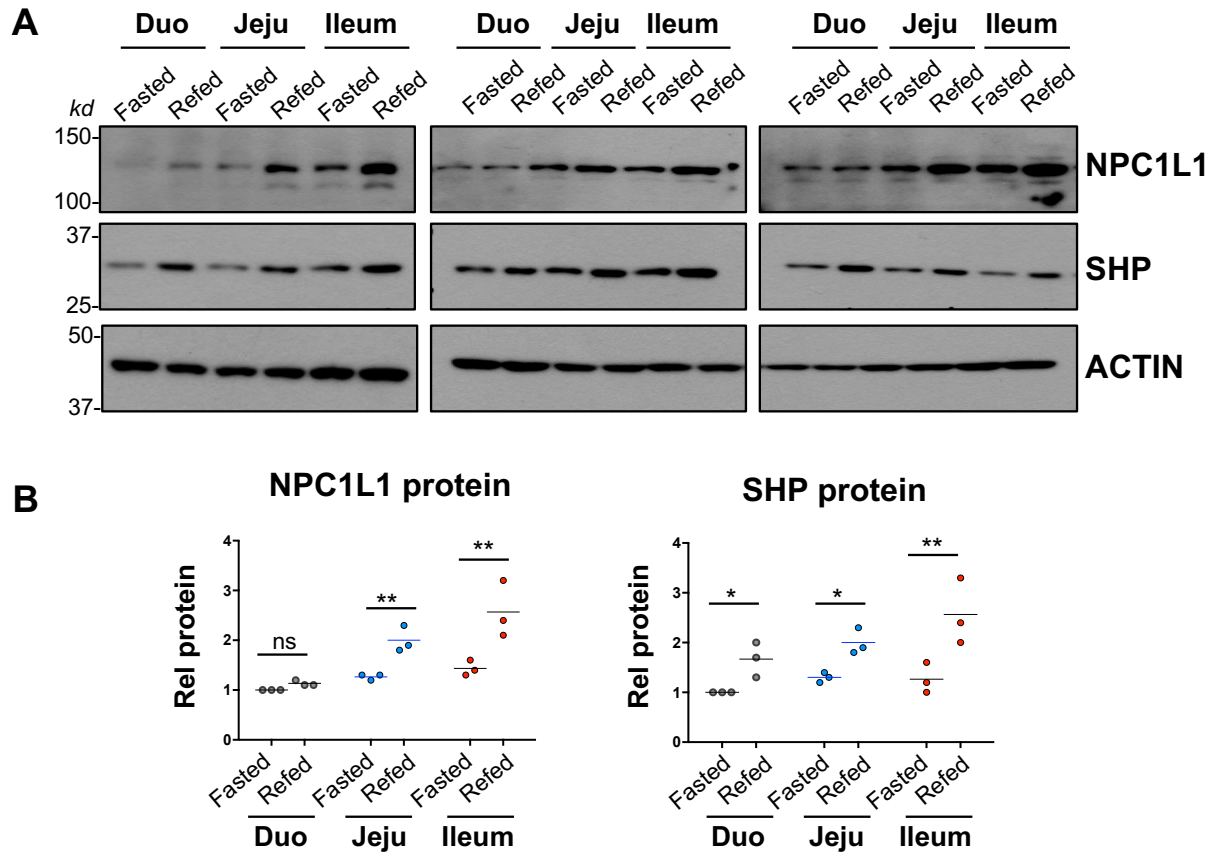


Supplemental Information

Materials and Methods

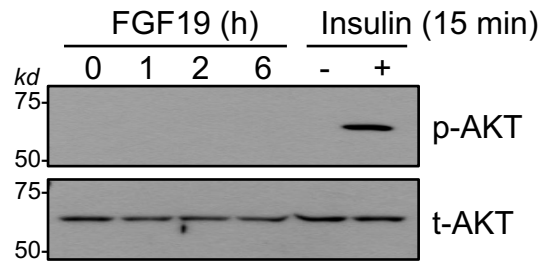
Reagents. Antibodies for SHP (sc-30169, H-160) and SREBF2 (sc-0563) were purchased from Santa Cruz Biotechnology; for NPC1L1 (LS-B506) from LifeSpan BioSciences, Inc.; and for p-ERK (#9101), ERK (#4695), AKT (#4685), and p-AKT (#4060) from Cell Signaling Technology, Inc. SHP antibody specific for phospho-Thr-55-SHP (p-T55-SHP) was produced commercially (Abmart, Inc.) and its use and specificity have been described in our previous studies^{11, 15, 20}. RNA SMARTpool for SREBF2 was purchased from GE Healthcare, Dharmacon. For cholesterol absorption assays, [¹⁴C]cholesterol (ARC0857) and [³H]sitosterol (ART1173) were purchased from American Radiolabeled Chemicals, Inc.

Supplementary Figures

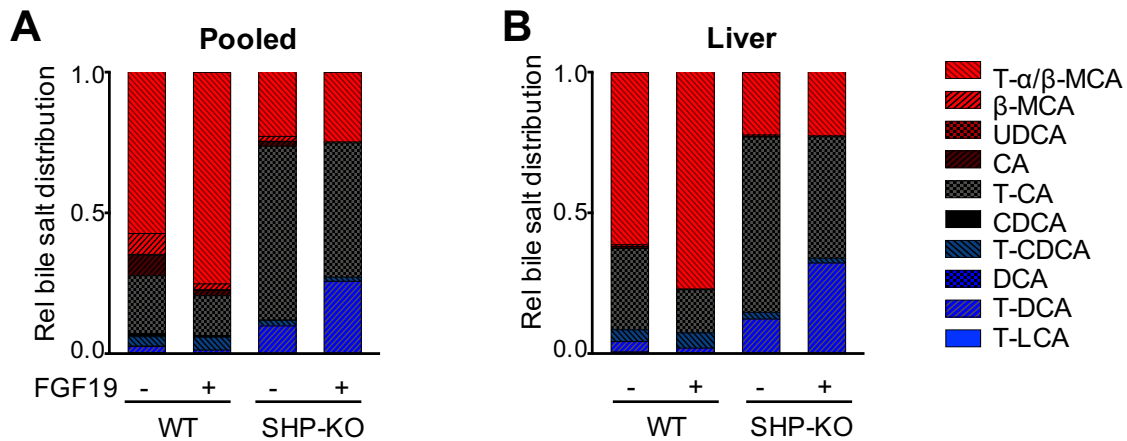


Supplementary Figure 1. Effects of fasting and refeeding on intestinal expression of NPC1L1 and SHP in WT mice. (A-B) WT mice ($n=3$) were fasted overnight and refed for 6 h, and protein levels in the duodenum (Duo), jejunum (Jeju), and ileum were measured. **(A)** NPC1L1 protein levels were detected by immunoblot (IB). **(B)** Protein levels normalized to actin with values for Duo, fasted set to 1 as measured by Image J software (v1.52e). Statistical significance was determined by one-way ANOVA with the FDR post-test, (SEM, $n=3$ to 5, * $P < 0.05$, ** $P < 0.01$, NS, statistically not significant).

IB: AKT phosphorylation  HT29 cell line



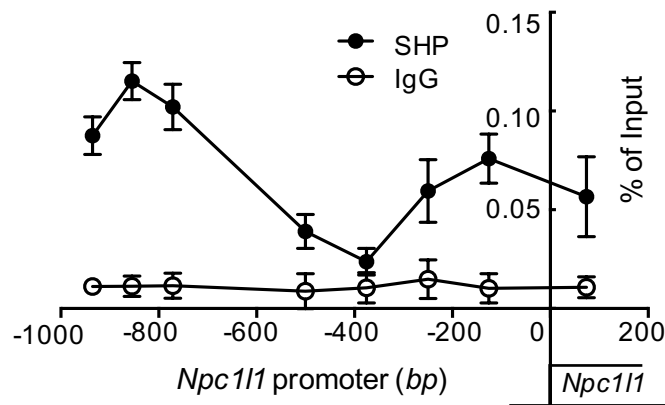
Supplementary Figure 2. Insulin signal-induced phosphorylation of AKT in human intestinal HT29 cells. HT29 cells were serum-starved overnight and treated with FGF19 or insulin for the indicated times. Phosphorylated AKT (p-AKT) and total AKT (t-AKT) was detected by immunoblot (IB).



Supplementary Figure 3. Effects of 1-week treatment of FGF19 on BA composition in WT and SHP-KO mice. WT and SHP-KO mice were treated daily with vehicle or FGF19 for 7 days and then caged individually. Mice were fasted overnight and refed for 24 h. **(A-B)** BA compositions were measured in the intestine, liver, and gallbladder pooled together **(A)** and in the liver **(B)**, and the stacked bar charts show the relative levels of the individual bile acids.



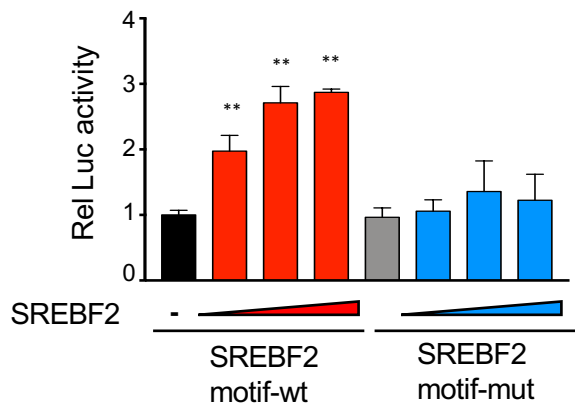
ChIP: SHP



Supplementary Figure 4. SHP occupancy is increased at the *Npc111* promoter by FGF19 treatment. WT mice were fasted overnight and injected with 1 mg/kg FGF19 via tail vein 1 h before sacrifice. SHP occupancy, using pooled jejunum and ileum tissues, was determined by ChIP assay for eight regions within +74 bp to -935 bp of *Npc111* promoter, (SEM, n=6).



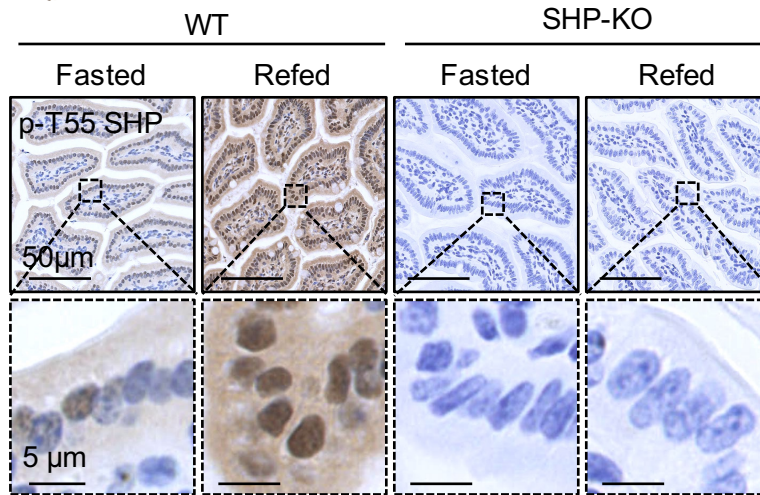
Npc111-Luc (HT29) (-721/-966bp)



Supplementary Figure 5. SREBF2 mediates transactivation of intestinal *Npc111* expression. HT29 cells were transfected with plasmids as indicated for 48 h, and luciferase activity was measured and normalized to β -galactosidase activity. Statistical significance was determined by one-way ANOVA with the FDR, (SEM, n=5, **P < 0.01).

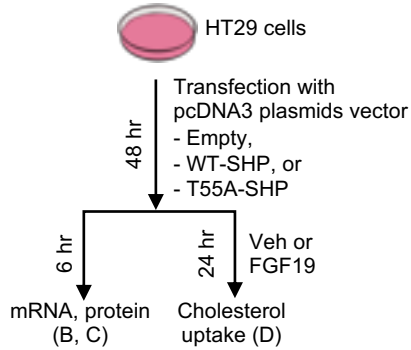


IHC: p-T55 SHP

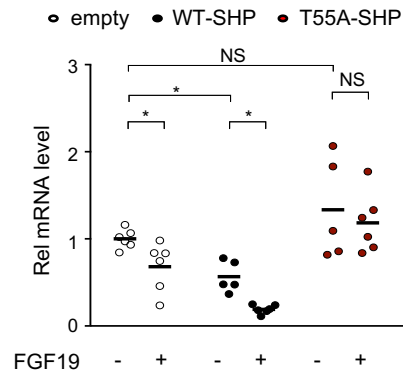


Supplementary Figure 6. Effects of FGF19-induced phosphorylation of SHP at Thr-55 in mouse intestine. WT and SHP-KO mice were fasted overnight and refed for 6 h and p-T55-SHP was detected by immunohistochemistry (IHC) in sections of the jejunum.

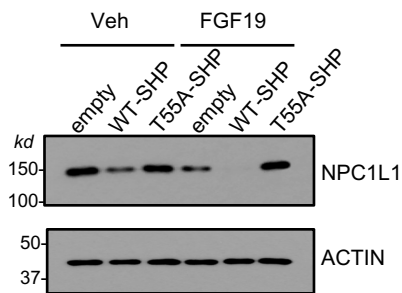
A SHP phosphorylation studies in HT29 cells (B-D)



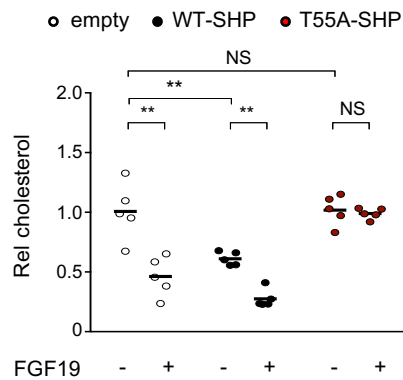
B NPC1L1 mRNA



C IB: NPC1L1 protein



D Cholesterol uptake



Supplementary Figure 7. FGF19 signal-induced phosphorylation of SHP at Thr-55 is important for inhibition of NPC1L1 expression and cholesterol uptake in human intestinal HT29 cells. (A) HT29 cells were transfected with expression plasmids for wild-type SHP (WT-SHP) or the phosphorylation defective mutant of SHP (T55A-SHP) for 48 h. (B-C) Levels of *NPC1L1* mRNA (B) or protein (C) after treatment with 50 ng/ml FGF19 for 6 h measured by RT-qPCR or IB, respectively. (D) HT29 cells were treated with 50 ng/ml FGF19 and fluorescently-tagged cholesterol was added to the medium for 24 h, and free cholesterol levels were determined by measuring the fluorescence intensity of the cells with excitation at 485 nm and emission at 535 nm as described in Methods. (B, D) Statistical significance was determined by two-way ANOVA with the FDR post-test, (SEM, n=5-6, *P <0.05, **P <0.01, NS, statistically not significant).

Supplementary Table 1

A List of mouse gene primer sequences for RT-qPCR

Definition	Sense primer	Anti-sense primer
<i>36b4</i>	CGACATCACAGAGCAGGC	CACCGAGGCAACAGTTGG
<i>Npc1l1</i>	GCAAGGTGATCAGGAGGTTGA	ATCCTCATCCTGGGCTTTGC
<i>Acat2</i>	GGAGATCCACCTTTCTGTGC	TCAATGGGAAACCGAGAGAC
<i>Abca1</i>	CAGTTAAGGCTGCTGCTGTG	TTGTTTCGTAGGGTGGGTAGC
<i>Hmgcr</i>	TGTCCTTGATGGCAGCCTT	AAGCTGCCTTCTTGGTGCA
<i>Insig1</i>	GAGGTGTCACAGTGGGAAA	CCACTCTGAACCATGTGCT
<i>Acly</i>	TGTTGACATTGGAGCCCTC	GATACAGCCCTTGCTTCAG
<i>Asbt</i>	CATGACCACTTGCTCCACAC	AATCGTTCCCGAGTCAACC
<i>Osta</i>	TGGACCCTGGAAGACATA	TAACCACTGATAAGGCTGAG
<i>Ostb</i>	ATCTTGATGACTCCATAATG	GTCTTTCTCTTTCAACTCA
<i>Npc1l1 (pre-mRNA)</i>	TTCCTGGCTCTGGGATGG	GAGGCACCAAGGAGTAGCC
<i>NPC1L1 (human)</i>	GTGTATGGCTCTGCCCTTG	AGGTGGAAGGTGATGTCCAG
<i>Fgf15</i>	GTTTCACCGCTCCTTCTTTG	CATCCTCCACCATCCTGAAC

B List of mouse gene primer sequences for CHIP q-PCR

Definition	Sense primer	Anti-sense primer
<i>Npc1l1 (+25/+123)</i>	ATCCCAGAGCCAGGAAGTG	GCTGCCTTAATGTGCAAACCTC
<i>Npc1l1 (-73/-178)</i>	GCCATTCCATCTCCTCCTTC	CCCGGTTGGCTCTAACTACC
<i>Npc1l1 (-190/-310)</i>	GAGCTGTTCTCTGCGAGAC	GAGGCGATGCGTTAGACTG
<i>Npc1l1 (-304/-447)</i>	TCGCCTCTTCAGATCAACATC	TCTGGTCCTGTTCCCTGTTAG
<i>Npc1l1 (-429/-572)</i>	AACAGGGAAACAGGACCAGAG	CAGGTTGGGTGGGACTTG
<i>Npc1l1 (-661/-881)</i>	AAGGGAAGCAGGTGATGTTG	GGACCTTGGCCTCTATTGC
<i>Npc1l1 (-817/-892)</i>	TAGGCAGGGAACAAGAGAGG	CAGGGAGCAACAAGGGAAG
<i>Npc1l1 (-897/-973)</i>	CCACCCAGTCCTCTTCTTGTC	GGATACTTGTCTCAGGGTCTGC
<i>Fgf15 (1900/2000)</i>	CCTGCCTGGTGGCTCTGTCTC	GGATAATCCGCAACTCCTCCCGCC